

# Rich Coordination of Nd<sup>3+</sup> in Mg<sub>2</sub>Nd<sub>13</sub>(BO<sub>3</sub>)<sub>8</sub>(SiO<sub>4</sub>)<sub>4</sub>(OH)<sub>3</sub>, Derived from High-Pressure/High-Temperature Conditions

Shijun Wu,<sup>†,‡</sup> Philip Kegler,<sup>†</sup> Shuao Wang,<sup>§</sup> Astrid Holzheid,<sup>†</sup> Wulf Depmeier,<sup>†</sup> Thomas Malcherek,<sup>⊥</sup> Evgeny V. Alekseev,<sup>\*,||</sup> and Thomas E. Albrecht-Schmitt<sup>\*,§</sup>

<sup>†</sup>Institut für Geowissenschaften, Universität zu Kiel, 24118 Kiel, Germany

<sup>‡</sup>Guangzhou Institute of Geochemistry, Chinese Academy of Sciences, 510640 Guangzhou, China

<sup>§</sup>Department of Chemistry and Biochemistry and Department of Civil Engineering and Geological Sciences, University of Notre Dame, South Bend, Indiana 46556, United States

<sup>⊥</sup>Mineralogisch-Petrographisches Institut, Universität Hamburg, 20146 Hamburg, Germany

<sup>||</sup>Forschungszentrum Jülich GmbH, Institute for Energy and Climate Research (IEK-6), 52428 Jülich, Germany

## Supporting Information

**ABSTRACT:** A neodymium borosilicate, Mg<sub>2</sub>Nd<sub>13</sub>(BO<sub>3</sub>)<sub>8</sub>(SiO<sub>4</sub>)<sub>4</sub>(OH)<sub>3</sub> (**MgNdBSi-1**), was obtained from a high-temperature (1400 °C), solid-state reaction under high-pressure conditions (4.5 GPa). **MgNdBSi-1** contains six different types of Nd<sup>3+</sup> coordination environments with three different ligands: BO<sub>3</sub>, SiO<sub>4</sub>, and OH groups. Mg<sup>2+</sup> cations are only bond to BO<sub>3</sub> groups and form porous two-dimensional layers based on 12-membered ring fragments. Surprisingly, the OH groups are retained at high temperature and reside at the center of Mg–BO<sub>3</sub> rings.

The synthetic and structural chemistry of Ln<sup>3+</sup> (Ln = lanthanide) and An<sup>3+</sup> (An = actinide) are quite similar.<sup>1</sup> Ln<sup>3+</sup> elements are often used as surrogates of An<sup>3+</sup> (Pu<sup>3+</sup>, Am<sup>3+</sup>, and Cm<sup>3+</sup>) in different systems.<sup>2</sup> One of the most important issues facing countries equipped with nuclear industries is the behavior of the actinides in nuclear waste repositories.<sup>3</sup> Borosilicate, boroaluminate, and borophosphate glasses are widely used for vitrification of nuclear waste in several countries (United States, Germany, France, United Kingdom, Belgium, Russia, et al.).<sup>4</sup> These glasses have complex cationic and anionic contents, including the presence of actinides in a variety of valence states.<sup>4,5</sup> Recently, we demonstrated the possibility of actinide complexation and crystalline material formation in the form of pure borates, borate phosphate, or boroaluminates. These phases were derived from different reaction conditions [hydrothermal, flux, or high-pressure/high-temperature (HP/HT) hydrothermal reactions], and the actinides can adopt a variety of valence states (from 3+ to 6+).<sup>6</sup> The behavior of actinides/lanthanides in such systems under extreme conditions (high pressures and high temperatures) is essentially unknown. Despite the recent systematic investigations of the behavior of lanthanides in pure borate systems under extreme conditions, multianionic systems are primarily represented by natural minerals and mineral-like materials.<sup>7</sup>

For our study, we chose the system Mg<sup>2+</sup> (up to 6 wt % in borosilicate glasses)–Nd<sub>2</sub>O<sub>3</sub> (surrogate of Am<sup>3+</sup> and Cm<sup>3+</sup>)–H<sub>3</sub>BO<sub>3</sub>–SiO<sub>2</sub>. During exploration of this system under extreme

conditions (1400 °C and 4.5 GPa), a new complex borosilicate, Mg<sub>2</sub>Nd<sub>13</sub>(BO<sub>3</sub>)<sub>8</sub>(SiO<sub>4</sub>)<sub>4</sub>(OH)<sub>3</sub> (**MgNdBSi-1**), was obtained.<sup>8</sup> The structure and optical properties of this phase were determined using single-crystal X-ray diffraction and spectroscopic measurements.

**MgNdBSi-1** possesses a very complex crystal structure, as shown in Figure 1. It forms a dense three-dimensional

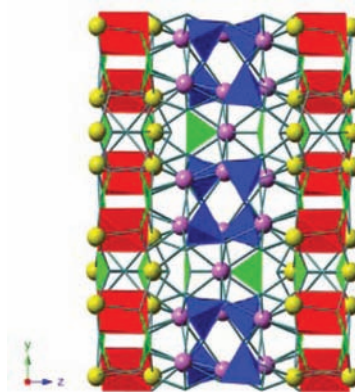


**Figure 1.** View of the **MgNdBSi-1** crystal structure. Nd atoms are shown in yellow and violet (see the text for details), magnesium polyhedra in red, boron triangles in green, and silicate tetrahedra in blue.

framework based on Nd<sup>3+</sup> and Mg<sup>2+</sup> cationic centers linked by BO<sub>3</sub> triangles and SiO<sub>4</sub> tetrahedra.

The overall structure can be separated into two parts. In the first part, Nd<sup>3+</sup> cations are coordinated with BO<sub>3</sub> triangles, SiO<sub>4</sub> tetrahedra, and OH groups. The Nd atoms from this portion are shown in Figure 1. In the second part, all Nd atoms are only connected to BO<sub>3</sub> and SiO<sub>4</sub> groups (shown in violet in Figure 1). The main fragment of the first part is a porous two-dimensional (2D) layer parallel to (001) (Figure 2). The layers are formed by Mg<sup>2+</sup> cations and BO<sub>3</sub> triangles. Each Mg atom is coordinated by six BO<sub>3</sub> groups, three on top

**Received:** February 2, 2012

**Published:** March 9, 2012

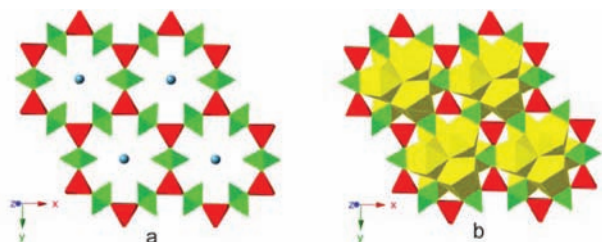


**Figure 2.** 2D layer parallel to (001) in the structure of **MgNdBSi-1**: (a) layer structure and OH group positions; (b) layer with Nd polyhedra. Nd atoms are shown in yellow, Mg atoms in red, and B atoms in green, and OH groups are light-blue spheres.

and three on the bottom of  $\text{MgO}_6$  trigonal prisms. A single unit of the Mg/B layer has a “wheel”-like shape and counts 18 members, 6 of which are  $\text{MgO}_6$  prisms and the other 12 of which are  $\text{BO}_3$  triangles. If one only considers the  $\text{BO}_3$  groups from one side of the Mg/B layer (up or down), then this layer is based upon 12-membered rings. Such an internal structure makes the layers pseudo-hexagonal.

The Mg/B layer is approximately 2.7 Å thick and slightly corrugated in both (100) and (010) projections. Only three of the  $\text{BO}_3$  groups from each side of the “wheel” point at the pore center; the remaining three are directed in the opposite direction. The Mg–O bond lengths range from 2.020(3) to 2.114(3) Å.

Four symmetrically independent B atoms (out of a total of six in the **MgNdBSi-1** structure) reside in the Mg/B layer. The interatomic distances in the  $\text{BO}_3$  groups are quite standard and range from 1.365(4) to 1.398(8) Å. The pore size is approximately  $5 \times 5$  Å (measured from terminal atoms of the  $\text{BO}_3$  groups). The geometrical centers of the described pores are occupied by OH groups (Figure 2a). These groups surprisingly remain stable and noncondensed during high-temperature heating. Apparently, the high pressures used in the synthesis of **MgNdBSi-1** increase the stability of the OH groups. There are three independent OH groups in each pore. One of them (O25) is in the center of the “wheel”. The other two OH groups are approximately 1 Å above and below the Mg/B layer surface (O20 and O21). All OH groups are only connected with  $\text{Nd}^{3+}$  cations, which fill the rest of the free space in the pores (Figure 2b). Each pore contains six Nd atoms (Nd1, Nd2, Nd3, and Nd4); three of them are on one side, and the other three are on another side. Topologically, each triplet is an equilateral triangle rotated by  $60^\circ$  with respect to each other.

A polyhedral representation shows a propeller-like projection of Nd-based polyhedra (Figure 2b) in the [001] plane. All Nd atoms residing within Mg/B layers are coordinated to both borate and orthosilicate, with CN 9 (Figure 3a,b), and form a complex cluster through Nd–OH–Nd bridges (Figure 3c). There are two different coordination environments of the Nd atoms in the first (yellow) part of **MgNdBSi-1**. The main difference between them is the number of  $\text{SiO}_4$  groups. In the first type (Figure 3a), there are only one  $\text{SiO}_4$  tetrahedron and five  $\text{BO}_3$  triangles surrounding the  $\text{Nd}^{3+}$  cation. In the second type (Figure 3b), one of the  $\text{BO}_3$  groups is substituted by a  $\text{SiO}_4$  unit. The Nd–O bond lengths are in the range from 2.416(5) to 2.789(6) Å. The shortest and longest bonds are connecting Nd to O20 and O21 and to O25, respectively. The bond distance variation can be rationalized by investigating the Nd–OH cluster (Figure 3c). O20 and O21 only have

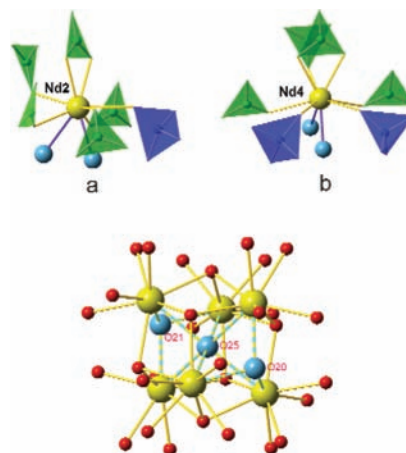


**Figure 3.** Local environment of the Nd sites in the first part of the **MgNdBSi-1** structure (a and b) and the structure of a Nd-based cluster within 2D layers (c). Nd atoms are shown in yellow,  $\text{BO}_3$  groups in green,  $\text{SiO}_4$  groups in blue, OH groups in light blue, and O atoms in red.

interactions with three Nd atoms, and in order to satisfy the bond valence sum on the O atoms, they have to be closer than O25, which interacts with all six surrounding Nd atoms. Here it is an interesting point that all groups are separated by their nature: the OH group is near OH, and  $\text{SiO}_4$  groups are close to  $\text{SiO}_4$ . The same tendency occurs in the “violet” part of **MgNdBSi-1**.

The second, “violet”, part of the **MgNdBSi-1** structure is not as diverse as the first one. However, this part demonstrates four different coordination environments for the Nd atoms with clearly tracked evolution (Figure 4).

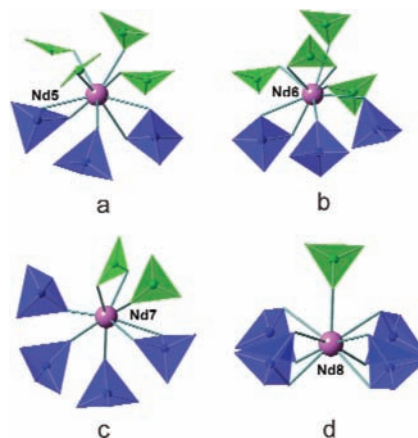


**Figure 4.** Local environment of Nd sites in the second part of the **MgNdBSi-1** structure. Nd atoms are shown in violet,  $\text{BO}_3$  groups in green, and  $\text{SiO}_4$  in blue.

Nd5 and Nd6 have CN 9 and are surrounded by four  $\text{BO}_3$  groups and three  $\text{SiO}_4$  units (Figure 4a,b). Two of the three  $\text{SiO}_4$  groups chelate Nd5, and all  $\text{BO}_3$  groups are monodentate. There are also two chelating groups around the Nd6 site, but these contrast with the Nd5 environment in that they are of a different nature; one is  $\text{BO}_3$ , and the other is  $\text{SiO}_4$ . The Nd–O bond lengths are in the range from 2.382(3) to 2.846(3) Å. Nd7 has CN 8, and this is the lowest coordination number among Nd sites in **MgNdBSi-1**. This site is surrounded by six oxo groups including four  $\text{SiO}_4$  and two  $\text{BO}_3$  (Figure 4c). Two of

them are chelating, one orthosilicate and one borate group. The interatomic distances are shorter than those in the previously described Nd sites and range from 2.309(3) to 2.682(3) Å. The final point of Nd environment evolution is the Nd8 site. It is surrounded only by five oxo groups, and only one of them is BO<sub>3</sub>. All four SiO<sub>4</sub> tetrahedra chelate Nd8, forming a NdO<sub>8</sub> tetragonal prism (Figure 4c). The prism has one cap donated from a BO<sub>3</sub> unit. The Nd–O distances in the square prism are quite close, from 2.548(3) to 2.609(2) Å. The capping O atom has a rather short distance of 2.365(3) Å.

The environment evolution of cations in the structure of MgNdBSi-1 is quite interesting. If one goes from the central plane of the 2D Mg/B layer to the central plane of the “violet” part [both are parallel to (001)], a change in the BO<sub>3</sub>/SiO<sub>4</sub> ratios from 5:1 to 1:4 will be observed in the Nd environment. Thus, in the “yellow” part, the structure of MgNdBSi-1 is more similar to pure neodymium borates, but in the “violet” part, it resembles pure neodymium silicates.

Nd<sup>3+</sup> is 4f<sup>3</sup> with a <sup>4</sup>I<sub>9/2</sub> ground state, and its f–f transitions have been assigned.<sup>10,11</sup> The absorption spectrum of MgNdBSi-1 was obtained from a twinned crystal using a microspectrophotometer and is shown in Figure S3 in the Supporting Information. We have used Carnall's analysis of the absorption spectrum of Nd<sup>3+</sup> to assign transitions for MgNdBSi-1 (Figure S3 in the Supporting Information). Although a variety of coordination environments are found for Nd<sup>3+</sup> in MgNdBSi-1, the spectrum is very similar to much simpler Nd compounds because the 4f orbitals are essentially nonbonding.<sup>10,11</sup> This compound emits in the near-IR as expected for Nd<sup>3+</sup> (see the Supporting Information).

## ■ ASSOCIATED CONTENT

### ■ Supporting Information

X-ray crystallographic file in CIF format, an Fourier transform IR spectrum, a fluorescence spectrum, a UV–vis–near-IR spectrum, and energy-dispersive X-ray analysis data. This material is available free of charge via the Internet at <http://pubs.acs.org>.

## ■ AUTHOR INFORMATION

### ■ Corresponding Author

\*E-mail: [e.alekseev@fz-juelich.de](mailto:e.alekseev@fz-juelich.de) (E.V.A.); [talbrecl@nd.edu](mailto:talbrecl@nd.edu) (T.E.A.-S.).

### ■ Notes

The authors declare no competing financial interest.

## ■ ACKNOWLEDGMENTS

We are grateful for financial support provided by Deutsche Forschungsgemeinschaft within Research Project DE 412/43-1 and by the Heavy Elements Chemistry Program, U.S. Department of Energy, under Grant DE-SC0002215, and to the Helmholtz Association for support within Project VH-NG-815.

## ■ REFERENCES

(1) (a) Allen, P. G.; Bucher, J. J.; Shuh, D. K.; Edelstein, N. M.; Craig, I. *Inorg. Chem.* **2000**, *39* (3), 595–601. (b) Jensen, M. P.; Bond, A. H. *J. Am. Chem. Soc.* **2002**, *124* (33), 9870–9877. (c) Gannaz, B.; Antonio, M. R.; Chiarizia, R.; Hill, C.; Cote, G. *Dalton Trans.* **2006**, *38*, 4553–4562. (d) Beneš, O.; Popa, K.; Reuscher, V.; Zappia, A.; Staicu, D.; Konings, R. J. M. *J. Nucl. Mater.* **2011**, *418*, 182–185. (e) Raison, P. E.; Jardin, R.; Bouëxière, D.; Konings, R. J. M.; Geisler, T.; Pavel, C. C.; Rebizant, J.; Popa, K. *Phys. Chem. Miner.* **2008**, *35*, 603–609.

(f) Ni, Y.; Hughes, J. M.; Mariano, A. N. *Am. Mineral.* **1995**, *80*, 21–26. (g) Podor, R.; Cuney, M.; Trung, C. N. *Am. Mineral.* **1995**, *80*, 1261–1268.

(2) (a) Villarreal, R.; Spall, D. *Selection of Actinide Chemical Analogues for WIPP Tests: Potential Nonradioactive Sorbing and Nonsorbing Tracers for Study of Ion Transport in the Environment*; Los Alamos National Laboratory: Los Alamos, NM, 1998. (b) Kim, C.-W.; Wronkiewicz, D. J.; Finch, R. J.; Buck, E. C. *J. Nucl. Mater.* **2006**, *353* (3), 147–157. (c) Pieper, H.; Bosbach, D.; Panak, P. J.; Rabung, T.; Fanghanel, T. *Clays Clay Miner.* **2006**, *54* (1), 45–53. (d) Stumpf, T.; Curtius, H.; Walther, C.; Dardenne, K.; Ufer, K.; Fanghanel, T. *Environ. Sci. Technol.* **2007**, *41* (9), 3186–3191. (e) Tan, X. L.; Fan, Q. H.; Wang, X. K.; Grambow, B. *Environ. Sci. Technol.* **2009**, *43* (9), 3115–3121. (f) Horlait, D.; Claparède, L.; Clavier, N.; Szenknect, S.; Dacheux, N.; Ravau, J.; Podor, R. *Inorg. Chem.* **2011**, *50*, 7150–7161. (g) Clavier, N.; Dacheux, N. *Inorg. Chem.* **2006**, *45*, 220–229. (h) Terra, O.; Dacheux, N.; Audubert, F.; Podor, R. *J. Nucl. Mater.* **2006**, *352*, 224–232. (i) Dacheux, N.; Clavier, N.; Robisson, A.-C.; Terra, O.; Audubert, F.; Lartigue, J.-É.; Guy, C. C. *R. Chimie* **2004**, *7*, 1141–1152.

(3) (a) Ewing, R. C. *Elements* **2006**, *2* (6), 331–334. (b) Pirlat, V. J. *Nucl. Mater.* **2001**, *298* (1–2), 47–54. (c) World Nuclear Association, <http://world-nuclear.org/info/inf21.html>. (d) Ojovan, M. I.; Lee, W. E. *Metall. Mater. Trans. A* **2011**, *42*, 837–851. (e) Ewing, R. C. *Proc. Natl. Acad. Sci. U.S.A.* **1999**, *99*, 3432–3439.

(4) (a) Commission on Geosciences, Environment and Resources. *Glass as a Waste Form and Vitrification Technology: Summary of an International Workshop*; National Academy of Sciences: Washington, DC, 1996. (b) International Atomic Energy Agency. *Spent Fuel and High Level Waste: Chemical Durability and Performance under Simulated Repository Conditions*; International Atomic Energy Agency: Vienna, Austria, 2007.

(5) Mtingwa, S. K. Feasibility of transmutation of radioactive elements. In *An international spent nuclear fuel storage facility-Exploring a Russian site as a prototype: Proceedings of an international workshop*; Schweitzer, G. E., Sharber, A. C., Eds.; The National Academies Press: Washington, DC, 2005; pp 30–49.

(6) (a) Wang, S.; Alekseev, E. V.; Depmeier, W.; Albrecht-Schmitt, T. E. *Chem. Commun.* **2011**, *47* (39), 10874–10885. (b) Wu, S.; Wang, S.; Diwu, J.; Depmeier, W.; Malcherek, T.; Alekseev, E. V.; Albrecht-Schmitt, T. E. *Chem. Commun.* **2012**, DOI: 10.1039/C2CC17517G. (c) Wu, S.; Beermann, O.; Wang, S.; Holzheid, A.; Depmeier, W.; Malcherek, T.; Modolo, G.; Alekseev, E. V.; Albrecht-Schmitt, T. E. *Chem.—Eur. J.* **2012**, in press.

(7) (a) Huppertz, H.; von der Eltz, B. *J. Am. Chem. Soc.* **2002**, *124* (32), 9376–9377. (b) Knyrim, J. S.; Roessner, F.; Jakob, S.; Johrendt, D.; Kinski, I.; Glaum, R.; Huppertz, H. *Angew. Chem., Int. Ed.* **2007**, *46* (47), 9097–9100. (c) Huppertz, H. *Chem. Commun.* **2011**, *47* (1), 131–140.

(8) A detailed synthetic procedure can be found in the Supporting Information. In a typical synthesis, a mixture of MgO, Nd<sub>2</sub>O<sub>3</sub>, H<sub>3</sub>BO<sub>3</sub>, and SiO<sub>2</sub> was ground and placed in a platinum capsule (outer diameter, 4.4 mm; inner diameter, 4 mm; length, 8 mm). The capsule was sealed and set into the center of a 0.2-in.-diameter MgO spacer. The experiment was performed at a pressure of 4.5 GPa and in temperature range from 1400 to 700 °C using the piston cylinder module of a Vöggenreiter LP 1000-540/50.

(9) Crystallographic data for MgNdBSi-1: purple block, 0.2 × 0.15 × 0.1 mm, monoclinic, *M*<sub>r</sub> = 2813.60, *P*<sub>2</sub>/m, *Z* = 2, *a* = 9.1691(9) Å, *b* = 15.8763(10) Å, *c* = 11.7800(10) Å, β = 106.120(8)°, *V* = 1647.4(2) Å<sup>3</sup>, μ = 204.111 cm<sup>-1</sup>, no. of reflns = 58303/5186, *R*<sub>int</sub> = 0.0566, *R*<sub>1</sub> = 0.0202 for *F*<sub>o</sub><sup>2</sup> > 2σ(*F*<sub>o</sub><sup>2</sup>), and w*R*<sub>2</sub> = 0.0413 for all data.

(10) Judd, B. R. *Phys. Rev.* **1962**, *127* (3), 750–761.

(11) Carnall, W. T.; Fields, P. R.; Wybourne, B. G. *J. Chem. Phys.* **1965**, *42* (11), 3797–3806.